

AlScN as an electron blocking layer in blue light emitting diodes: A first look

Cite as: Appl. Phys. Lett. **128**, 093304 (2026); doi: [10.1063/5.0310893](https://doi.org/10.1063/5.0310893)

Submitted: 5 November 2025 · Accepted: 2 February 2026 ·

Published Online: 3 March 2026



View Online



Export Citation



CrossMark

Pierce Lonergan,^{1,a)}  Madhav Ramesh,¹  Shivali Agrawal,²  Debaditya Bhattacharya,¹  Thai-Son Nguyen,³ 
Vladimir Protasenko,¹  Henryk Turski,⁴  Huili Grace Xing,^{1,3,5}  and Debdeep Jena^{1,3,5,b)} 

AFFILIATIONS

¹School of Electrical and Computer Engineering, Cornell University, Ithaca, New York 14853, USA

²R.F. Smith School of Chemical and Biomolecular Engineering, Cornell University, Ithaca, New York 14853, USA

³Department of Materials Science and Engineering, Cornell University, Ithaca, New York 14853, USA

⁴Institute of High Pressure Physics, Polish Academy of Sciences, Sokotowska 29/37, Warsaw 01-142, Poland

⁵Kavli Institute at Cornell for NanoScale Science, Cornell University, Ithaca, New York 14853, USA

Note: This paper is part of the Special Topic on Frontiers in Nitride Semiconductors Research.

^{a)}Author to whom correspondence should be addressed: pal245@cornell.edu

^{b)}Electronic mail: djena@cornell.edu

ABSTRACT

Electron blocking layers (EBLs) are instrumental in visible light emitters based on nitride semiconductor heterostructures. AlScN (a) can be lattice-matched to GaN, (b) can be grown at GaN compatible conditions, and (c) offers favorable band offsets required for EBLs, but has not been used in light emitting devices to date. In this work, we test if lattice-matched AlScN can be integrated as an EBL layer in a blue light emitting diode (LED) pn junction heterostructure. We find that blue LED operation with peak electroluminescence (EL) at ~ 460 nm can indeed be realized with an AlScN EBL. In the LED with the AlScN EBL, we observe low reverse leakage current density, and ~ 6 nm lower full-width at half maximum of the EL peak compared to a control sample. Though the turn-on voltage of the AlScN EBL containing blue LED is high, this demonstration proves its feasibility and provides guidance for improved performance in the future.

Published under an exclusive license by AIP Publishing. <https://doi.org/10.1063/5.0310893>

AlScN is an upcoming semiconductor material that has shown significant promise in the vast phase space of semiconductor devices. Specifically, the material has found a strong niche in high-electron-mobility transistors (HEMTs) for RF applications,¹ bulk acoustic wave (BAW) resonators,² and multi-channel heterostructures.³ The listed applications stem from AlScN's unique properties, such as its strong piezoelectric behavior (15 pm/V for 18% Sc),⁴ high relative dielectric constant (10–20),⁵ and ferroelectric nature.^{6,7} In addition, AlScN is known to have a lattice-matched condition to GaN at approximately 9%–12% mole fraction of Sc.^{3,8,9} The lattice-matched condition of AlScN/GaN offers a way toward reducing defects related to strain. Coupling all the aforementioned properties with the fact that GaN and AlScN have compatible growth conditions, AlScN offers an interesting possibility for integration in light emitting devices.

Some concrete examples of the utilization of the unique properties of AlScN in photonics and optoelectronics include non-linear photonics,¹⁰ infrared detectors,¹¹ and Bragg reflectors.⁹ In contrast, AlScN

is yet to be used in an active light emitting device such as light emitting diodes (LEDs) and laser diodes (LDs). A natural point of insertion of AlScN in such devices is the electron blocking layer (EBL), which serves to block overflow of electrons from the active region quantum well(s) into the p-region, while simultaneously allowing for hole injection across it. To achieve this, an ideal EBL would possess a large conduction band offset with a negligible valence band offset.

Recently, Jin *et al.* have reported that the AlScN/GaN band alignment shifts from type I to type II past a Sc mole fraction of approximately 8% as measured by x-ray photoelectron spectroscopy (XPS).¹² For example, at a 12% Sc mole fraction, the AlScN/GaN heterojunction has a type II band offset, with a conduction band offset of $\Delta E_c = 2.68$ eV and valence band offset of $\Delta E_v = 0.14$ eV.¹² Typical AlGaN EBLs used in blue GaN LEDs, with $12\% \pm 4\%$ Al mole fraction, have type I band offset, with a conduction band offset of $\Delta E_c = 0.203$ eV and valence band offset of $\Delta E_v = -0.125$ eV.^{13–16} In addition to the band offsets, lattice-matched AlScN offers the possibility of eliminating strain in the EBL.

Lattice-matched AlInN has also been explored for EBLs in blue LEDs.¹⁵ Compared to the extreme change in the growth conditions required to integrate AlInN with GaN/InGaN heterostructures, AlScN offers the opportunity to grow the entire heterostructure with much lower temperature variation.^{17,18} For AlScN, the growth conditions, especially that for the lattice-matched condition, are compatible with GaN as AlScN can be grown from 450 to 800 °C with stable wurtzite phase purity.^{19,20}

Motivated by the above arguments, in this work we explore the integration of AlScN as an EBL in a blue LED heterostructure by epitaxial growth. For comparison, we use a blue LED heterostructure without an EBL. The two LED samples were grown by plasma-assisted molecular beam epitaxy (MBE) using a Veeco Gen10 MBE reactor on *c*-plane, Ga-polar bulk n-GaN substrates. The growth surface of the films was monitored *in situ* using a KSA Instruments RHEED paired with a Staib electron gun operated at 14.5 kV, 1.45 A. The active nitrogen was provided using a RF plasma source with a flow rate of 1.05 sccm and 200 W RF power. Scandium, aluminum, indium, gallium, silicon, and magnesium were supplied using separate effusion cells.

The heterostructure layers for both devices are shown in Figs. 1(a) and 1(b). A 200 nm thick n-GaN layer was grown under metal-rich conditions with a silicon doping concentration of $\sim 1 \times 10^{19} \text{ cm}^{-3}$ at a substrate temperature measured by a thermocouple of 700 °C following a Ga polish of the underlying substrate at 750 °C. Following the n-GaN layer, the InGaN quantum well (18% In) and barriers (7% In) were grown under In-rich conditions at 650 °C with targeted thicknesses of 3 and 10 nm, respectively. For the sample containing the AlScN EBL [Fig. 1(b)], the AlScN was grown under nitrogen-rich conditions at a III/V ratio of ~ 0.8 with a substrate temperature of 650 °C and projected

thickness of 15 nm as typical for AlGaIn EBLs that range from 15 to 20 nm.^{14,16,21} Both samples were then capped with a metal-rich p-GaN layer of aimed 150 nm thickness at a Mg doping concentration of $\sim 4 \times 10^{19} \text{ cm}^{-3}$ and substrate temperature of 700 °C.

Figure 1(c) shows the predicted band offsets and bandgaps based on the AlScN Sc molar fraction of 12%. Using data from Jin *et al.*,¹² the conduction band and valence band offsets for AlScN/GaN heterojunction are 2.66 eV and 0.14 eV, respectively. Since the data were obtained from XPS, the valence band offset is measured directly. The conduction band offset was obtained from the known valence band offset and the bandgap of AlScN at 12% Sc mole fraction.¹² The bandgap for GaN is also shown with a value of 3.42 eV.^{22–24} Using the known electron affinity for GaN of 3.08 eV, the conduction band offset of 2.66 eV, and the vacuum level as a reference, the AlScN electron affinity for 12% mole fraction Sc is deduced to be 0.42 eV.²⁵

The crystal structure and thicknesses of the LED structures were determined by x-ray diffraction (XRD). The strain of the LED structures was analyzed by reciprocal space mapping (RSM). XRD and RSM were collected with a PANalytical Empyrean system with Cu K α 1 radiation.

The measured thicknesses and compositions of the layers in Figs. 1(a) and 1(b) derived from XRD fitting shown in Fig. 2(a) are relatively close to the targeted values in the growth. The InGaN barriers reduce the polarization-induced Stark effect in the well for improved electron and hole wave function overlap.^{26,27} Additionally, the barriers enable continuous growth from the bottom to the top of the active region under In-rich conditions, ensuring smooth interfaces with the well. The InGaN quantum well thickness for both structures is measured to be 4 nm. The AlScN EBL thickness was about 1 nm thicker than the targeted 16 nm. Finally, there was a slight variation in the two p-GaN layers with the AlScN containing sample having a p-GaN thickness of 130.0 nm and the AlScN-free sample having 138.8 nm thick p-GaN. Overall, the composition and thickness values obtained from XRD, as shown in Fig. 2(a), confirm that the two samples have comparable designs besides the AlScN EBL layer.

Figure 2(b) shows the reciprocal space map (RSM) for the LED samples containing the AlScN EBL. All peaks shown are associated with the $-1\ 0\ 5$ asymmetric peak. The vertically aligned peaks in the RSM scan suggest AlScN and InGaN layers are all strained to the GaN peak, indicating low density of defects expected in a coherently strained film.²⁸ Because the InGaN quantum well thickness is only 4 nm thick, we do not observe its asymmetric peak.

For the fabrication of LEDs, circular 20 nm thick palladium pads with varying diameters (from 10 to 400 μm) were processed. The palladium was patterned and deposited by photolithography, followed by electron beam evaporation and liftoff. The backside of the samples were silver pasted to a silicon substrate with blanket deposited Ti/Au. The diodes were probed in a vertical device configuration, with the Pd electrode serving as the anode and the Ti/Au electrode, which contacts the n-GaN substrate from the backside as the cathode. Current–voltage (*I*–*V*) data were collected using a Keithley 4200A SCS parameter analyzer. For electroluminescence measurements, current was sourced from a Keithley 2636B sourcemeter, and light was collected with an Acton SP2500 monochromator from the top of the sample.

Figures 3(a) and 3(b) show the linear and log-scale *I*–*V* curves of the two LED samples. Accordingly, the turn-on voltage of the AlScN

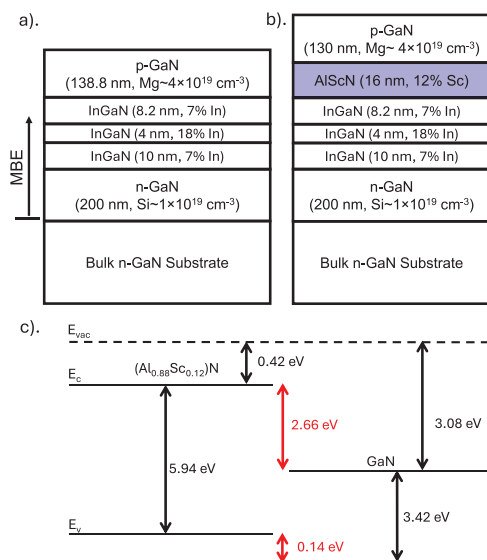


FIG. 1. (a) The material stack for the as-grown LED samples not containing the AlScN EBL with material thicknesses and compositions from XRD. (b) The material stack for the as-grown LED samples, containing the AlScN EBL, with material thicknesses and compositions determined by XRD. (c) Though there is a range of experimentally reported energy offsets, recent XPS measured values for AlScN are shown in this figure.

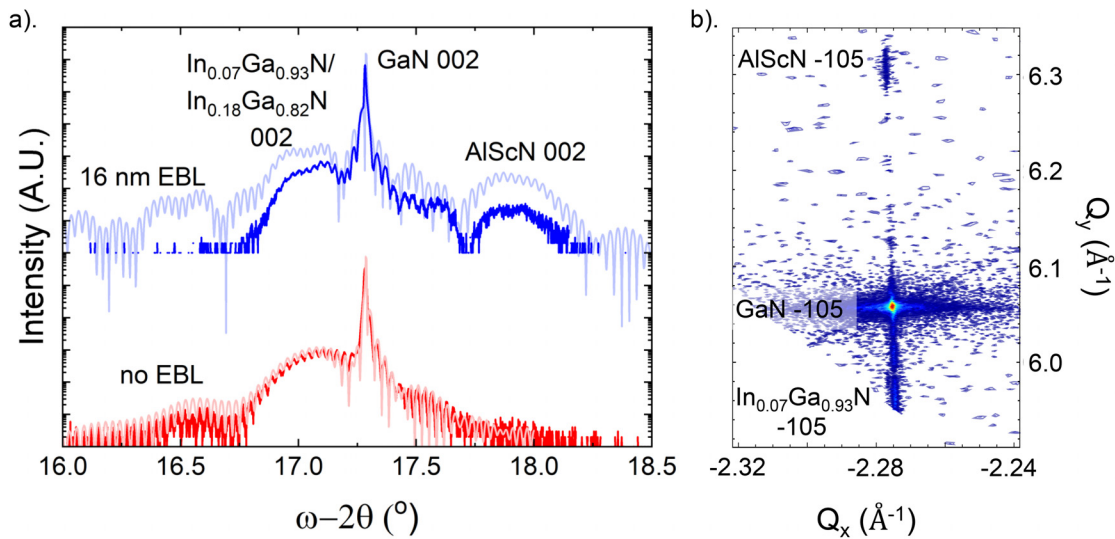


FIG. 2. (a) Symmetric $\omega-2\theta$ XRD of the 002 peak for both LED samples with the simulated results for each sample superimposed as a semi-transparent line. (b) Reciprocal space map of the sample containing the AlScN EBL illustrating a fully strained structure.

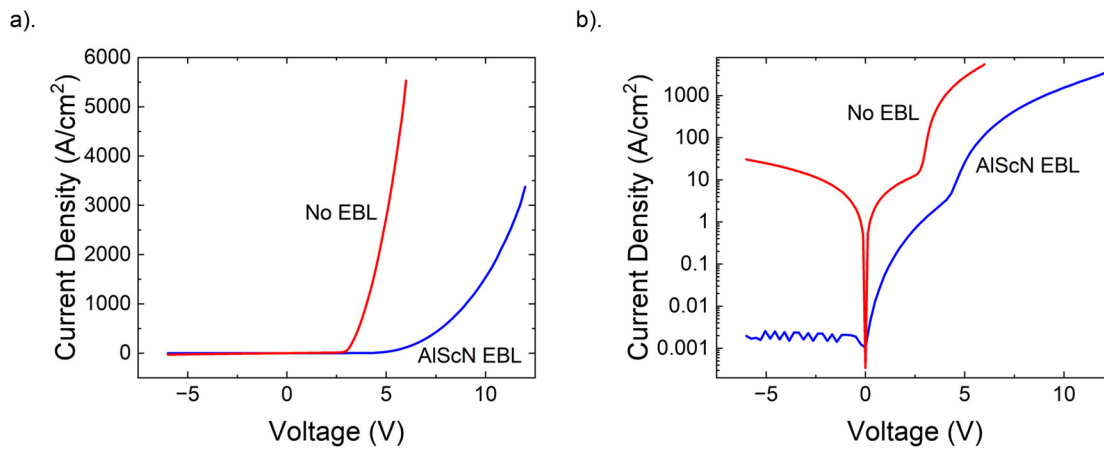


FIG. 3. (a) Linear I-V for both LED samples. (b) Log-scale I-V for both LED samples.

EBL sample as presented in Fig. 3(b) is ~ 4.32 V, while the control sample has a turn-on voltage of ~ 2.76 V. This difference in turn-on voltage can be attributed to the addition of the AlScN EBL layer. The LED containing the AlScN EBL has a higher turn-on voltage than that of standard LEDs with AlGaN EBLs, where the turn-on voltage is between 2.5 and 3 V.^{16,21}

The AlScN EBL LED has a higher turn-on voltage because (a) it is undoped and (b) has a large polarization field opposing hole injection as seen in the energy band diagram under forward bias in Fig. 1S of the supplementary material. It can be inferred that the increased turn-on voltage does not originate from the p-contact, as the contact resistivity values extracted from transfer length method (TLM) measurements were 2.29×10^{-2} and $1.03 \times 10^{-2} \Omega \text{cm}^2$ for the control sample and AlScN EBL sample, respectively. Doping the AlScN layer offers a solution to both problems, but doping of AlScN has been

problematic due to the nitrogen-rich growth conditions.^{20,29} Future studies can use the newly developed surfactant-assisted epitaxy of AlScN to address the doping bottleneck and lower the turn-on voltage.³⁰ In addition, the growth of the p-GaN layer directly on the AlScN EBL resulted in rougher surface morphology with droplet-like features. It ought to be possible to remove such undesired features via introduction of transition layers in the future.

From Fig. 3(b), the reverse leakage current density of the sample containing the AlScN EBL is $0.002 \text{ A}/\text{cm}^2$ at -5 V. In contrast, the reverse leakage current density of the sample without the AlScN EBL is $30 \text{ A}/\text{cm}^2$ at -5 V as normalized by the area of the top electrode. Both current densities were measured using the same contact diameter of $30 \mu\text{m}$. Because similar structures without EBL have been realized with much lower leakage currents by similar growth methods,³¹ it would be incorrect to attribute the reduced leakage current entirely to the

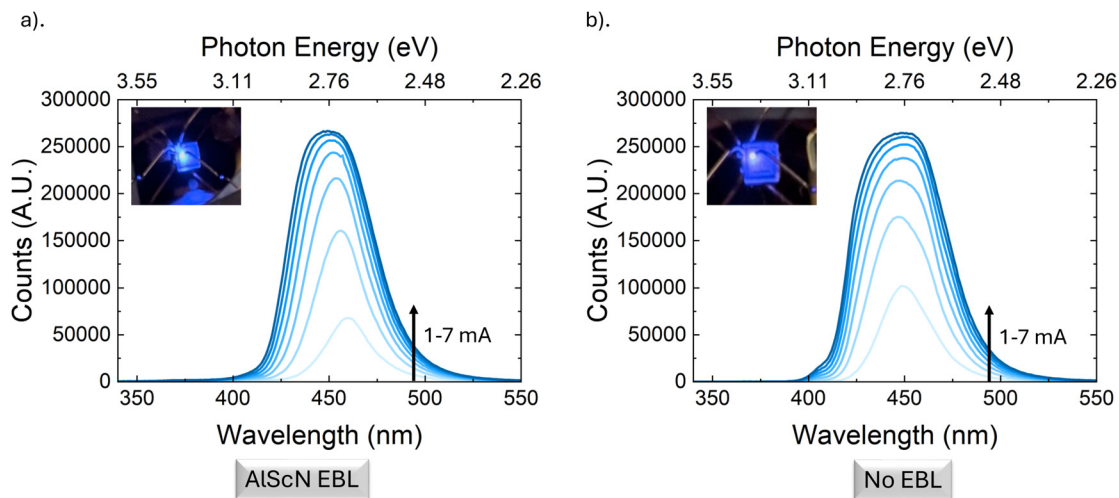


FIG. 4. (a) Electroluminescence of the sample with an AlScN EBL with total current injection ranging from 1 to 7 mA in steps of 1 mA, with an inset of the device under forward operation. (b) Electroluminescence of the sample without an AlScN EBL with total current injection ranging from 1 to 7 mA in steps of 1 mA, with an inset of the device under forward operation.

introduction of the AlScN EBL. Nevertheless, the AlScN EBL prevents the flow of minority electrons from the p-GaN to the n-GaN at a reverse bias due to the high conduction band barrier that electrons encounter.

Figures 4(a) and 4(b) show the top-collected electroluminescence (EL) of the two LED samples with an inset of the two devices under similar forward bias conditions. In both cases, the total injected current was increased from 1 to 7 mA in steps of 1 mA. From a qualitative point of view, the luminescence appears to be quite similar in both cases. This proves that AlScN is a viable EBL for blue LEDs. However, the EL curves at identical current input show that the intensity of light for the sample containing an AlScN EBL is lower than that of the sample without the EBL. However, the EL full-width half maximum (FWHM) for the AlScN EBL sample is narrower than that for the AlScN-free sample with an average FWHM difference of ~ 6.2 nm, indicating stronger carrier confinement.

For both samples, we can see a clear blue shift in the EL peak as carrier injection is increased. The blue shift is due to the electron screening of the polarization charge, as is typical for polar LEDs.³² Recent computational work has suggested that electron screening is only part of the reason for the blue shift, with exchange–correlation effects and phase space filling of carriers in disordered potentials caused by alloy variation in the InGaN wells also contributing.³³ The peak wavelength blue shifts of the samples with and without an AlScN EBL are from 460 to 450 nm and 449 to 446 nm, respectively. For 1 mA injection current, the peak EL wavelength is higher for that with the AlScN EBL. Despite XRD showing near identical active region compositions, there is a 10 nm EL peak difference between the two devices. This possibly originates from the induced Stark effect in the InGaN well by the AlScN layer due to the large polarization of AlScN.

In summary, we have demonstrated a blue light emitting diode containing an AlScN EBL by designing the layer in such a way that we maintain a near-lattice-matched Sc mole fraction whose band offset with GaN was recently reported as type II.¹² The presence of the AlScN EBL causes an increase in the overall turn-on voltage from 2.76

to 4.32 V due to the large series resistance introduced by the AlScN. The large series resistance of AlScN is in part due to the lack of p-doping, and the introduction of a polarization-induced barrier for holes from the p-GaN to the active region. However, the LED with an AlScN EBL showed narrower FWHMs of the peak wavelength with an average difference of ~ 6.2 nm. In addition, the AlScN EBL LED showed a on-off ratio of $\sim 6 \times 10^4$ at ± 6 V. In the future, additional research will be conducted to optimize the AlScN EBL structure, such as the possibility of p-type doping AlScN using a newly developed surfactant epitaxy technique to reduce the series resistance.³⁰ Such a solution could help to lower the turn-on voltage by lowering the series resistance and polarization barrier for holes.

See the [supplementary material](#) for the energy band diagram of both LEDs under forward bias at the same current density value of 50 A/cm^2 .

This work made use of the Cornell Center for Materials Research shared instrumentation facility. This work was supported in part by SUPREME, one of seven centers in JUMP 2.0, a Semiconductor Research Corporation (SRC) program sponsored by DARPA.

AUTHOR DECLARATIONS

Conflict of Interest

The authors have no conflicts to disclose.

Author Contributions

Pierce Lonergan: Conceptualization (equal); Data curation (equal); Formal analysis (equal); Investigation (equal); Methodology (equal); Writing – original draft (equal); Writing – review & editing (equal). **Madhav Ramesh:** Data curation (equal); Formal analysis (equal); Investigation (equal); Methodology (equal); Writing – review & editing (equal). **Shivali Agrawal:** Data curation (equal); Formal

analysis (equal); Investigation (equal); Methodology (equal); Writing – review & editing (equal). **Debaditya Bhattacharya:** Data curation (equal); Formal analysis (equal); Investigation (equal); Methodology (equal); Writing – review & editing (equal). **Thai-Son Nguyen:** Data curation (equal); Formal analysis (equal); Investigation (equal); Methodology (equal); Writing – review & editing (equal). **Vladimir Protasenko:** Data curation (equal); Investigation (equal); Methodology (equal); Writing – review & editing (equal). **Henryk Turski:** Conceptualization (equal); Writing – review & editing (equal). **Huili Grace Xing:** Funding acquisition (equal); Project administration (supporting); Resources (equal); Supervision (supporting); Writing – review & editing (equal). **Debdeep Jena:** Funding acquisition (lead); Project administration (lead); Resources (equal); Supervision (lead); Writing – review & editing (equal).

DATA AVAILABILITY

The data that support the findings of this study are available from the corresponding author upon reasonable request.

REFERENCES

- J. Casamento, K. Nomoto, T. S. Nguyen, H. Lee, C. Savant, L. Li, A. Hickman, T. Maeda, J. Encomendero, V. Gund, A. Lal, J. C. M. Hwang, H. G. Xing, and D. Jena, “FerroHEMTs: High-current and high-speed all-epitaxial AlScN/GaN ferroelectric transistors,” in International Electron Devices Meeting (IEDM), 2022.
- K. Umeda, H. Kawai, A. Honda, M. Akiyama, T. Kato, and T. Fukura, “Piezoelectric properties of ScAlN thin films for piezo-MEMS devices,” in *IEEE 26th International Conference on Micro Electro Mechanical Systems (MEMS)* (IEEE, 2013), pp. 733–736.
- T.-S. Nguyen, C. Savant, A. Asteris, H. G. Xing, and D. Jena, “Transport properties of lattice-matched AlScN/GaN single- and multichannel heterostructures,” *Appl. Phys. Lett.* **127**, 102106 (2025).
- J. Casamento, C. S. Chang, Y.-T. Shao, J. Wright, D. A. Muller, H. G. Xing, and D. Jena, “Structural and piezoelectric properties of ultra-thin $\text{Sc}_x\text{Al}_{1-x}\text{N}$ films grown on GaN by molecular beam epitaxy,” *Appl. Phys. Lett.* **117**, 112101 (2020).
- J. Casamento, H. Lee, T. Maeda, V. Gund, K. Nomoto, L. van Deurzen, W. Turner, P. Fay, S. Mu, C. G. Van de Walle, A. Lal, H. G. Xing, and D. Jena, “Epitaxial $\text{Sc}_x\text{Al}_{1-x}\text{N}$ on GaN exhibits attractive high-K dielectric properties,” *Appl. Phys. Lett.* **120**, 152901 (2022).
- S. Fichtner, N. Wolff, F. Lofink, L. Kienle, and B. Wagner, “AlScN: A III-V semiconductor based ferroelectric,” *J. Appl. Phys.* **125**, 114103 (2019).
- J. Casamento, V. Gund, H. Lee, K. Nomoto, T. Maeda, B. Davaji, M. J. Asadi, J. Wright, Y.-T. Shao, D. A. Muller, A. Lal, H. (Grace) Xing, and D. Jena, “Ferroelectricity in polar ScAlN/GaN epitaxial semiconductor heterostructures,” [arXiv:2105.10114](https://arxiv.org/abs/2105.10114) (2021).
- D. V. Dinh, J. Lähnemann, L. Geelhaar, and O. Brandt, “Lattice parameters of $\text{Sc}_x\text{Al}_{1-x}\text{N}$ layers grown on GaN(0001) by plasma-assisted molecular beam epitaxy,” *Appl. Phys. Lett.* **122**, 152103 (2023).
- L. van Deurzen, T.-S. Nguyen, J. Casamento, H. G. Xing, and D. Jena, “Epitaxial lattice-matched AlScN/GaN distributed Bragg reflectors,” *Appl. Phys. Lett.* **123**, 241104 (2023).
- J. Liu, P.-L. Thériault, S. Liu, D. Wang, W. Wu, Q. Wen, Z. Zhang, M. Soltani, M. Kira, S. Kéna-Cohen, and Z. Mi, “Second-order optical nonlinearities in ferroelectric ScAlN for quantum photonics,” in *IEEE Photonics Conference (IPC)*, 2023.
- G. Gopakumar, Z. U. Abidin, R. Kumar, B. Dzuba, T. Nguyen, M. J. Manfra, and O. Malis, “Conduction-band engineering of polar nitride semiconductors with wurtzite ScAlN for near-infrared photonic devices,” *J. Appl. Phys.* **135**, 165701 (2024).
- E. N. Jin, M. T. Hardy, A. L. Mock, J. L. Lyons, A. R. Kramer, M. J. Tadjer, N. Nepal, D. S. Katzer, and D. J. Meyer, “Band alignment of $\text{Sc}_x\text{Al}_{1-x}\text{N}$ /GaN hetero-junctions,” *ACS Appl. Mater. Interfaces* **12**, 52192–52200 (2020).
- D. R. Hang, C. H. Chen, Y. F. Chen, H. X. Jiang, and J. Y. Lin, “ $\text{Al}_x\text{Ga}_{1-x}\text{N}$ /GaN band offsets determined by deep-level emission,” *J. Appl. Phys.* **90**, 1887–1890 (2001).
- H. Turski, S. Bharadwaj, H. G. Xing, and D. Jena, “Polarization control in nitride quantum well light emitters enabled by bottom tunnel-junctions,” *J. Appl. Phys.* **125**, 203104 (2019).
- S. Choi, H. J. Kim, S.-S. Kim, J. Liu, J. Kim, J.-H. Ryou, R. D. Dupuis, A. M. Fischer, and F. A. Ponce, “Improvement of peak quantum efficiency and efficiency droop in III-nitride visible light-emitting diodes with an InAlN electron-blocking layer,” *Appl. Phys. Lett.* **96**, 221105 (2010).
- K.-H. Kim, S.-W. Lee, S.-N. Lee, and J. Kim, “Effect of p- $\text{Al}_x\text{Ga}_{1-x}\text{N}$ electron blocking layer on optical and electrical properties in GaN-based light emitting diodes,” *J. Vac. Sci. Technol., B* **30**, 061204 (2012).
- W. Terashima, S.-B. Che, Y. Ishitani, and A. Yoshikawa, “Growth and characterization of AlInN ternary alloys in whole composition range and fabrication of InN/AlInN multiple quantum wells by RF molecular beam epitaxy,” *Jpn. J. Appl. Phys., Part 2* **45**, L539 (2006).
- K. Jeganathan and M. Shimizu, “Importance of growth temperature on achieving lattice-matched and strained InAlN/GaN heterostructure by plasma-assisted molecular beam epitaxy,” *AIP Adv.* **4**, 097113 (2014).
- M. T. Hardy, E. N. Jin, N. Nepal, D. S. Katzer, B. P. Downey, V. J. Gokhale, D. F. Storm, and D. J. Meyer, “Control of phase purity in high scandium fraction heteroepitaxial ScAlN grown by molecular beam epitaxy,” *Appl. Phys. Express* **13**, 065509 (2020).
- M. T. Hardy, B. P. Downey, N. Nepal, D. F. Storm, D. S. Katzer, and D. J. Meyer, “Epitaxial ScAlN grown by molecular beam epitaxy on GaN and SiC substrates,” *Appl. Phys. Lett.* **110**, 162104 (2017).
- N.-C. Oh, J.-G. Lee, Y. Dong, T.-S. Kim, H.-J. Yu, and J.-H. Song, “Effect of p-AlGaIn electron blocking layers on the injection and radiative efficiencies in InGaIn/GaN light emitting diodes,” *Curr. Appl. Phys.* **15**, S7–S10 (2015).
- J. Wu, W. Walukiewicz, K. Yu, J. Ager III, S. Li, E. Haller, H. Lu, and W. J. Schaff, “Universal bandgap bowing in group-iii nitride alloys,” *Solid State Commun.* **127**, 411–414 (2003).
- N. Nepal, J. Li, M. Nakarmi, J. Lin, and H. Jiang, “Temperature and compositional dependence of the energy band gap of AlGaIn alloys,” *Appl. Phys. Lett.* **87**, 242104 (2005).
- A. Naito, K. Ueno, and H. Fujioka, “Heavy ge doping in gan via pulsed sputtering to tailor the optical bandgap energy,” *Phys. Status Solidi A* **221**, 2300990 (2024).
- P. Strak, P. Kempisty, K. Sakowski, and S. Krukowski, “*Ab initio* determination of electron affinity of polar nitride surfaces, clean and under Cs coverage,” *J. Vac. Sci. Technol., A* **35**, 021406 (2017).
- J. Xu, M. F. Schubert, A. N. Noemaun, D. Zhu, J. K. Kim, E. F. Schubert, M. H. Kim, H. J. Chung, S. Yoon, C. Sone, and Y. Park, “Reduction in efficiency droop, forward voltage, ideality factor, and wavelength shift in polarization-matched GaInN/GaN multi-quantum-well light-emitting diodes,” *Appl. Phys. Lett.* **94**, 011113 (2009).
- Y.-K. Kuo, J.-Y. Chang, M.-C. Tsai, and S.-H. Yen, “Advantages of blue InGaIn multiple-quantum well light-emitting diodes with InGaIn barriers,” *Appl. Phys. Lett.* **95**, 011116 (2009).
- A. E. Romanov, E. C. Young, F. Wu, A. Tyagi, C. S. Gallinat, S. Nakamura, S. P. DenBaars, and J. S. Speck, “Basal plane misfit dislocations and stress relaxation in III-nitride semipolar heteroepitaxy,” *J. Appl. Phys.* **109**, 103522 (2011).
- E. Haus, I. P. Smorchkova, B. Heying, P. Fini, C. Poblentz, T. Mates, U. K. Mishra, and J. S. Speck, “The role of growth conditions on the p-doping of GaN by plasma-assisted molecular beam epitaxy,” *J. Cryst. Growth* **246**, 55–63 (2002).
- P. Lonergan, T.-S. Nguyen, C. Savant, H. Turski, H. G. Xing, and D. Jena, “Indium surfactant assisted molecular beam epitaxy of AlScN,” *APL Mater.* **13**, 101103 (2025).
- Y. Cho, S. Bharadwaj, Z. Hu, K. Nomoto, U. Jahn, H. G. Xing, and D. Jena, “Blue (In,Ga)N light-emitting diodes with buried n^+p^+ tunnel junctions by plasma-assisted molecular beam epitaxy,” *Jpn. J. Appl. Phys., Part 1* **58**, 060914 (2019).
- J.-H. Ryou, P. D. Yoder, J. Liu, Z. Lochner, H. Kim, S. Choi, H. J. Kim, and R. D. Dupuis, “Control of quantum-confined Stark effect in InGaIn-based quantum wells,” *IEEE J. Sel. Top. Quantum Electron.* **15**, 1080–1091 (2009).
- N. Pant, X. Li, E. DeJong, D. Feezell, R. Armitage, and E. Kioupakis, “Origin of the injection-dependent emission blueshift and linewidth broadening of III-nitride light-emitting diodes,” *AIP Adv.* **12**, 125020 (2022).

AlScN as an Electron Blocking Layer in Blue Light-Emitting Diodes: A First Look

Pierce Lonergan,^{1, a)} Madhav Ramesh,¹ Shivali Agrawal,² Debaditya Bhattacharya,¹ Thai-Son Nguyen,³ Vladimir Protasenko,¹ Henryk Turski,⁴ Huili Grace Xing,^{1,3,5} and Debdeep Jena^{1,3,5,6}

¹⁾*School of Electrical and Computer Engineering, Cornell University, Ithaca, New York 14853, USA*

²⁾*R.F. Smith School of Chemical and Biomolecular Engineering, Cornell University, Ithaca, New York 14853, USA*

³⁾*Department of Materials Science and Engineering, Cornell University, Ithaca, New York 14853, USA*

⁴⁾*Institute of High Pressure Physics, Polish Academy of Sciences, Sokółowska 29/37, Warsaw, 01-142, Poland*

⁵⁾*Kavli Institute at Cornell for Nanoscale Science, Cornell University, Ithaca, New York 14853, USA*

⁶⁾*School of Applied and Engineering Physics, Cornell University, Ithaca, New York 14853, USA*

The supplementary material includes:

Figure S1 – Energy band diagram of both LEDs under forward bias at the same current density value of 50 A/cm².

^{a)}Electronic mail: pal245@cornell.edu

SUPPLEMENTARY INFORMATION

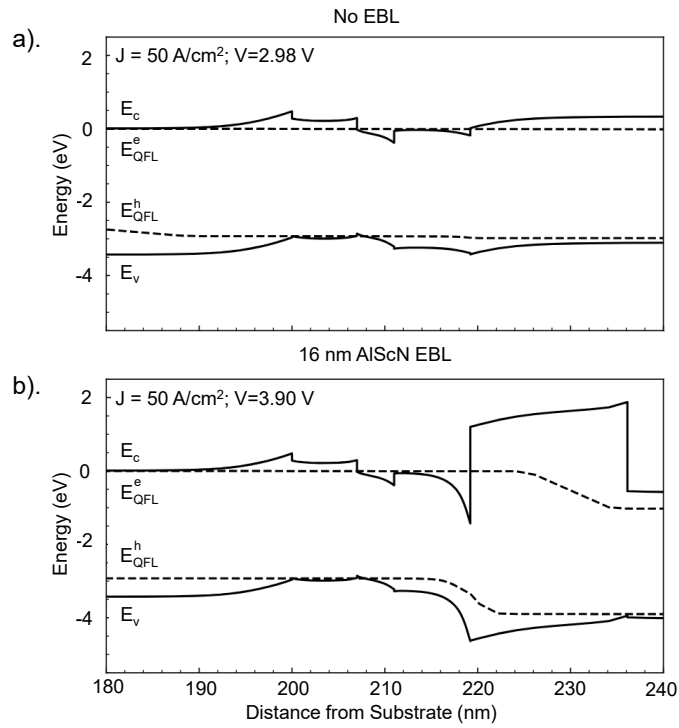


FIG. S1. (a) Energy band diagram for the LED without an AlScN EBL forward biased at 2.98 V giving a current density of 50 A/cm^2 . (b) Energy band diagram for the LED with an AlScN EBL forward biased at 3.90 V giving a current density of 50 A/cm^2 .